International Journal of Science and Advanced Innovative Research
ISSN: 2536-7315 (Print) 2536-7323 (Online)
Volume 5, Number 1, March, 2020
http://www.casirmediapublishing.com

THEORETICAL PREDICATION OF MASS DISTRIBUTION OF FRAGMENTS FOR ^{90}Kr AND ^{92}Kr

[1]E. W. Likta, [2]F. W. Burari & [2]I. Maina
[1]Department of Physics, University of Maiduguri, P.M.B 1069, Maiduguri, Borno State
[2]Department of Physics, Abubakar Tafawa Balewa University, Bauchi, P.M.B 0248, Bauchi
[1]Email: emmalikta2014@gmail.com

ABSTRACT
The study has been obtained theoretical that demonstrated the neutron-rich fragments are also produced in the deep inelastic transfer reactions occurring in the region between Coulomb barrier and Fermi energy regime. It has been achieved the applicability of multi-fragmentation in the transition region between Coulomb barrier and Fermi energy regime. The goal of this paper is to achieve the theoretical prediction of mass distribution of fragment for ^{90}Kr and ^{92}Kr. The theoretical reaction of ^{90}Kr and ^{92}Kr have been obtained. Collisions stages have been predicated. The results obtained are in agreement with the experimental data.
Key word: ^{90}Kr , ^{92}Kr, Coulomb, fragments, Hot and Cold

INTRODUCTION
Krypton is a chemical element with symbol Kr and atomic number 36. It is a member of group 18 (noble gases) elements, Krypton is from Ancient Greek name κρυπτός, translit and kryptos is the hidden one. A colorless, odorless, tasteless noble gas, krypton occurs in trace amounts in the atmosphere and is often used with other rare gases in fluorescent lamps. With rare exceptions, krypton is chemically inert. Krypton, like the other noble gases, is used in lighting and photography. Krypton light has many spectral lines and krypton plasma is useful in bright, high-powered gas lasers (krypton ion and excimer lasers), each of which resonates and amplifies a single spectral line. Krypton fluoride also makes a useful laser medium [1].

This agreement replaced the 1889 international prototype meter located in Paris, which was a metal bar made of a platinum -iridium alloy one of a series of standard meter bars, originally constructed to be one ten-millionth of a quadrant of the Earth's polar circumference [2]. This also obsolete the 1927 definition of the ångström based on the red cadmium spectral line, replacing it with 1 Å = 10 −10 m [3]. The krypton-86 definition lasted until the October 1983 conference, which redefined the meter as the distance that light travels in vacuum during $\frac{1}{299,792,458}s$ [4]. Krypton is characterized by several sharp

emission lines the strongest being green and yellow [5]. Krypton is one of the products of uranium fission [6]. Solid krypton is white and has a face-centered cubic crystal structure, which is a common property of all noble gases (except helium, which has a hexagonal close-packed crystal structure). Naturally occurring krypton in Earth's atmosphere is composed of five stable isotopes, plus one isotope (^{78}Kr) with such a long half-life that it can be considered stable. This isotope has the second-longest known half-life among all isotopes for which decay has been observed; it undergoes double electron capture to ^{78}Se. In addition, about thirty unstable isotopes and isomers are known [4]. Traces of ^{81}Kr, a cosmogenic nuclide produced by the cosmic ray irradiation of ^{80}Kr, also occur in nature: this isotope is radioactive with a half-life of 230,000 years. Krypton is highly volatile and does not stay in solution in near- surface water, but ^{81}Kr has been used for dating old (50,000–800,000 years) groundwater [5]. ^{85}Kr is an inert radioactive noble gas with a half-life of 10.76 years. It is produced by the fission of uranium and plutonium, such as in nuclear bomb testing and nuclear reactors. ^{85}Kr is released during the reprocessing of fuel rods from nuclear reactors. Concentrations at the North Pole are 30% higher than at the South Pole due to convective mixing [6]. Will obtained the characteristics of fragment mass, isotope distributions and the fragmentation mechanism. Also, the comparing results of both calculated and experimental.

MATERIALS AND METHOD

One may define the weight of the fragmentation probability of each event as follows:

$$W_j = \xi \exp\left(S_j(E^*, A, Z)\right) \quad (1)$$

Here ξ is the normalization constant, S_j is the entropy of each channel, E^* is the excitation energy, A is the mass number and Z is the charge number of the droplets. The free energy of a fragmentation can be defined in terms of the parameters of Bethe-Weizacker formula as a sum of the bulk, surface, Coulomb and symmetry energy terms as

$$F_{A,Z} = F^B_{A,Z} + F^S_{A,Z} + F^C_{A,Z} + F^{sym}_{A,Z} \quad (2)$$

Here $F^B_{A,Z} = \left(-W_0 - \frac{T^2}{\varepsilon_0}\right)A$ is the bulk term with the temperature T, the level density parameter ε_0 and the binding energy $W_0 = 16\,MeV$ for symmetric nuclear matter, $F^S_{A,Z} = B_0 A^{\frac{2}{3}}\left[\frac{(T_C^2 - T^2)}{(T_C^2 + T^2)}\right]^{\frac{5}{4}}$ is the surface energy with the surface

International Journal of Science and Advanced Innovative Research
ISSN: 2536-7315 (Print) 2536-7323 (Online)
Volume 5, Number 1, March, 2020
http://www.casirmediapublishing.com

energy term $B_0 = 18\ MeV$ and the critical temperature $T_C = 18\ MeV$, $E_{A,Z}^C = \frac{(c\ Z^2)}{A^{\frac{1}{3}}}$ is the Coulomb energy contribution with the Coulomb parameter c obtained in Wigner-Seitz approximation as $c = \left(\frac{3}{5}\right)\left(\frac{e^2}{r_0} - \left(\frac{\rho}{\rho_0}\right)^{\frac{1}{3}}\right)$, charge unit e, $r_0 = 1.17$ fm and the normal nuclear matter density $\rho_0 = 0.15\ fm^{-3}$ and $E_{A,Z}^{sym} = \gamma\frac{(A-2Z)^2}{A}$ is the symmetry term with the ground state value of the symmetry energy parameter $\gamma = 25\ MeV$.[7] The weight of the channel containing n particles with masses $mi = (i = 1, \dots, n)$ is given by

$$\Delta\Gamma_f^{mic} \propto \frac{S}{G}\left(\frac{V_f}{(2\pi\eta)^3}\right)^{n-1}\left(\frac{\prod_{i=1}^n m_i}{m_0}\right)^{\frac{3}{2}}\frac{(2\pi)^{\left(\frac{3}{2}\right)(n-1)}}{\Gamma\left(\frac{3}{2}(n-1)\right)}\left(E_{kin} - U_f^C\right)^{\left(\frac{3}{2}\right)n-\frac{5}{2}}$$

3

Where $m_0 = \sum_{i=1}^n m_i$ is the total mass, $S = \prod_{i=1}^n (2s_i + 1)$ is the spin degeneracy factor, $G = \prod_{J=1}^n n_j\ !$ is the particle identity factor with n_j the number of the jth particles, E_{kin} is the total kinetic energy of the fragments, and U_f^C is the Coulomb interaction energy of secondary cold particles.

RESULTS

The emission width of a particle j emitted from the compound nucleus (A, Z) is given by

$$\Gamma_j^{\,2} = \left(\sum_{i=1}^n \int_0^{E_{A,Z}^* - B_j - \varepsilon_j^{(i)}} \frac{\mu_j\, g_j^{(i)}}{\pi^2\,\eta^3}\ \sigma_j(E)\ \ \frac{\rho_{A'Z'}\left(E_{AZ}^* - B_j - E\right)}{\rho_{AZ}\left(E_{AZ}^*\right)}\right)^2$$

4

Where the summation is taken all over the states, $\varepsilon_j^i (i = 0, 1, \dots, n)$ is for the fragments j, $g_j^{(i)} = (2s^{(i)}\, j + 1)$ is the spin degeneracy factor of the excited state j, μ_j is the reduced mass, B_j is the separation energy, E_{AZ}^* is the excitation energy of the source and E is the kinetic energy of an emitted particle in the centre of mass frame.

Table 1a: Hot and Cold fragment for ^{90}Kr.

S/N	^{90}Kr Hot Fragment		^{90}Kr Cold Fragment	
	A	Multiplicity (Exponential)	A	Multiplicity (Exponential)
1	1	−0.65	2	−0.65
2	2	−1.45	3	−0.55

3	3	−1.55	4	−0.20
4	4	−1.35	5	−2.89
5	5	−1.00	6	−0.98
6	6	−1.10	7	−0.96
7	7	−1.20	8	−0.94
8	8	−1.25	9	−1.30
9	9	−1.30	10	−1.31
10	10	−1.31	11	−1.30
11	11	−1.40	12	−1.60
12	12	−1.45	13	$10^{-1.45}$
13	13	−1.50	14	−1.80
14	14	−1.55	15	−1.65
15	15	−1.70	16	−1.83
16	16	−1.75	17	−1.82
17	17	−1.81	18	−1.83
18	18	−1.82	19	−1.82
19	19	−1.85	20	−1.85
20	20	−1.86	21	−1.83
21	21	−1.88	22	−1.86
22	22	−1.89	23	−1.84
23	23	−1.90	24	−1.87
24	24	−1.92	25	−1.84
25	25	−1.93	26	−1.88
26	26	−1.94	27	−1.85
27	27	−1.95	28	−1.90
28	28	−1.96	29	−1.88
29	29	−1.97	30	−2.10
30	30	−1.98	31	−2.13
31	31	−1.99	32	−2.17
32	32	−2.00	33	−2.21
33	33	−2.01	34	−2.24
34	34	−2.06	35	−2.27
35	35	−2.10	36	−2.28
36	36	−2.14	37	−2.29
37	37	−2.18	38	−2.30
38	38	−2.20	39	−2.31

39	39	−2.24	40	−2.32
40	40	−2.28	41	−2.35
41	41	−2.31	42	−2.36
42	42	−2.33	43	−2.38
43	43	−2.36	44	−2.40
44	44	−2.39	45	−2.38
45	45	−2.40	46	−2.37
46	46	−2.48	47	−2.35
47	47	−2.46	48	−2.32
48	48	−2.48	49	−2.29
49	49	−2.50	50	−2.25
50	50	−2.47	51	−2.22
51	51	−2.45	52	−2.20
52	52	−2.42	53	−2.19
53	53	−2.40	54	−2.17
54	54	−2.37	55	−2.16
55	55	−2.33	56	−2.14
56	56	−2.31	57	−2.13
57	57	−2.27	58	−2.10
58	58	−2.23	59	−2.09
59	59	−2.20	60	−2.08
60	60	−2.18	61	−2.05
61	61	−2.15	62	−2.04
62	62	−2.13	63	−2.03
63	63	−2.11	64	−2.01
64	64	−2.07	65	−2.00
65	65	−2.01	66	−1.90
66	66	−2.00	67	−1.89
67	67	−1.99	68	−1.87
68	68	−1.97	69	−1.85
69	69	−1.94	70	−1.84
70	70	−1.93	71	−1.83
71	71	−1.91	72	−1.80
72	72	−1.90	73	−1.81
73	73	−1.89	74	−1.83
74	74	−1.87	75	−1.84

75	75	−1.85	76	−1.85
76	76	−1.83	77	−1.86
77	77	−1.80	78	−1.89
78	78	−1.80	79	−1.90
79	79	−1.80	80	−1.95
80	80	−1.80	81	−1.97
81	81	−1.80	82	−1.99
82	82	−1.80	83	−2.00
83	83	−1.80	84	−2.10
84	84	−1.80	85	−2.30
85	85	−1.80	86	−2.40
86	86	−1.80	87	−2.50
87	87	−1.80	88	−2.70
88	88	−1.80	89	−2.89
89	89	−1.80	90	−3.50
90	90	−1.98	-	-

Table 1b: Hot and Cold fragment ^{92}Kr.

S/N	^{92}Kr Hot Fragment		^{92}Kr Cold Fragment	
	A	Multiplicity (Exponential)	A	Multiplicity (Exponential)
1	2	−1.45	2	−0.65
2	3	−1.55	3	−0.55
3	4	−1.35	4	−0.20
4	5	−1.00	5	−2.89
5	6	−1.10	6	−0.98
6	7	−1.20	7	−0.96
7	8	−1.25	8	−0.94
8	9	−1.30	9	−1.30
9	10	−1.31	10	−1.31
10	11	−1.40	11	−1.30
11	12	−1.45	12	−1.60
12	13	−1.50	13	−1.81
13	14	−1.55	14	−1.80
14	15	−1.70	15	−1.65

15	16	−1.75	16	−1.83
16	17	−1.81	17	−1.82
17	18	−1.82	18	−1.83
18	19	−1.85	19	−1.82
19	20	−1.86	20	−1.85
20	21	−1.88	21	−1.83
21	22	−1.89	22	−1.86
22	23	−1.90	23	−1.84
23	24	−1.92	24	−1.87
24	25	−1.93	25	−1.84
25	26	−1.94	26	−1.88
26	27	−1.95	27	−1.85
27	282	−1.96	28	−1.90
28	29	−1.97	29	−1.88
29	30	−1.98	30	−2.10
30	31	−1.99	31	−2.13
31	32	−2.00	32	−2.17
32	33	−2.01	33	−2.21
33	34	−2.06	34	−2.24
34	35	−2.10	35	−2.27
35	36	−2.14	36	−2.28
36	37	−2.18	37	−2.29
37	38	−2.20	38	−2.30
38	39	−2.24	39	−2.31
39	40	−2.28	40	−2.32
40	41	−2.31	41	−2.35
41	42	−2.33	42	−2.36
42	43	−2.36	43	−2.38
43	44	−2.39	44	−2.40
44	45	−2.40	45	−2.39
45	46	−2.40	46	−2.39
46	47	−2.42	47	−2.38
47	48	−2.48	48	−2.37
48	49	−2.46	49	−2.35
49	50	−2.48	50	−2.32
50	51	−2.50	51	−2.29

51	52	−2.47	52	−2.25
52	53	−2.45	53	−2.22
53	54	−2.42	54	−2.20
54	55	−2.40	55	−2.19
55	56	−2.37	56	−2.17
56	57	−2.33	57	$10^{-2.16}$
57	58	−2.31	58	−2.14
58	59	−2.27	59	−2.13
59	60	−2.23	60	−2.10
60	61	−2.20	61	−2.09
61	62	−2.18	62	−2.08
62	63	−2.15	63	−2.05
63	64	−2.13	64	−2.04
64	65	−2.11	65	−2.03
65	66	−2.07	66	−2.01
66	67	−2.01	67	−2.00
67	68	−2.00	68	−1.90
68	69	−1.99	69	−1.89
69	70	−1.97	70	−1.87
70	71	−1.94	71	−1.85
71	72	−1.93	72	−1.84
72	73	−1.91	73	−1.83
73	74	−1.90	74	−1.80
74	75	−1.89	75	−1.81
75	76	−1.87	76	−1.83
76	77	−1.85	77	−1.84
77	78	−1.83	78	−1.85
78	79	−1.80	79	−1.86
79	80	−1.80	80	−1.89
80	81	−1.80	81	−1.90
81	82	−1.80	82	−1.95
82	83	−1.80	83	−1.97
83	84	−1.80	84	−1.99
84	85	−1.80	85	−2.00
85	86	−1.80	86	−2.10
86	87	−1.80	87	−2.30

International Journal of Science and Advanced Innovative Research
ISSN: 2536-7315 (Print) 2536-7323 (Online)
Volume 5, Number 1, March, 2020
http://www.casirmediapublishing.com

87	88	−1.80	88	−2.40
88	89	−1.80	89	−2.50
89	90	−1.80	90	−2.70
90	91	−1.80	91	−2.89
91	92	−1.98	92	−3.50

Table 2: Theoretical and Experimental Results for ^{90}Kr if $Z=30$

	If $Z=30$							
	Theoretical Result				Experimental Result			
	^{90}Kr		^{92}Kr		^{90}Kr		^{92}Kr	
S/N	A	mb	A	Mb	A	mb	A	mb
1	61	-2.9	63	-0.6	59	-1.6	61	-0.4
2	62	-1.6	64	0.1	60	-0.7	62	0.0
3	63	-0.7	65	0.3	61	-0.2	63	0.3
4	64	0.2	66	0.4	62	0.2	64	0.4
5	65	0.6	67	0.3	63	0.3	65	0.4
6	66	0.6	68	0.4	64	0.4	66	0.3
7	67	0.3	69	0.2	65	0.3	67	0.9
8	68	0.2	70	0.0	66	0.1	68	-0.2
9	69	-0.1	71	-0.1	67	0.0	69	-0.4
10	70	-0.2	72	-0.4	68	-0.5	70	-0.6
11	71	-0.7	73	-0.8	69	-0.7	71	-0.8
12	72	-0.6	74	-0.7	70	-0.9	72	-0.9
13	73	-0.8	75	-0.8	71	-1.0	73	-1.4
14	74	-0.7	76	-0.7	72	-1.9	74	-1.7
15	75	-0.9	77	-0.8	73	-2.6	75	-2.6
16	76	-0.9	78	-0.9	-	-	76	-2.9
17	-	-	-	-	-	-	77	-3.7
18	-	-	-	-	-	-	78	-3.9

Table 3: Theoretical and Experimental Results for ^{92}Kr if $Z=29$

	^{92}Kr if $Z=29$			
	Theoretical Result		Experimental Result	
S/N	A	mb	A	mb
1	59	-2.6	58	-0.3

2	60	-1.0	59	0.1
3	61	0.1	60	0.4
4	62	0.3	61	0.8
5	63	0.5	62	0.4
6	64	0.4	63	0.2
7	65	0.3	64	0.1
8	66	0.1	65	0.0
9	67	0.0	66	-0.3
10	68	-0.7	67	-0.5
11	69	-0.8	68	-0.9
12	70	-0.9	69	-1.4
13	71	-0.9	70	-1.9
14	72	-1.4	71	-2.0
15	73	-1.1	72	-2.2
16	74	-1.5	73	-2.5
17	75	-1.7	-	-

International Journal of Science and Advanced Innovative Research
ISSN: 2536-7315 (Print) 2536-7323 (Online)
Volume 5, Number 1, March, 2020
http://www.casirmediapublishing.com

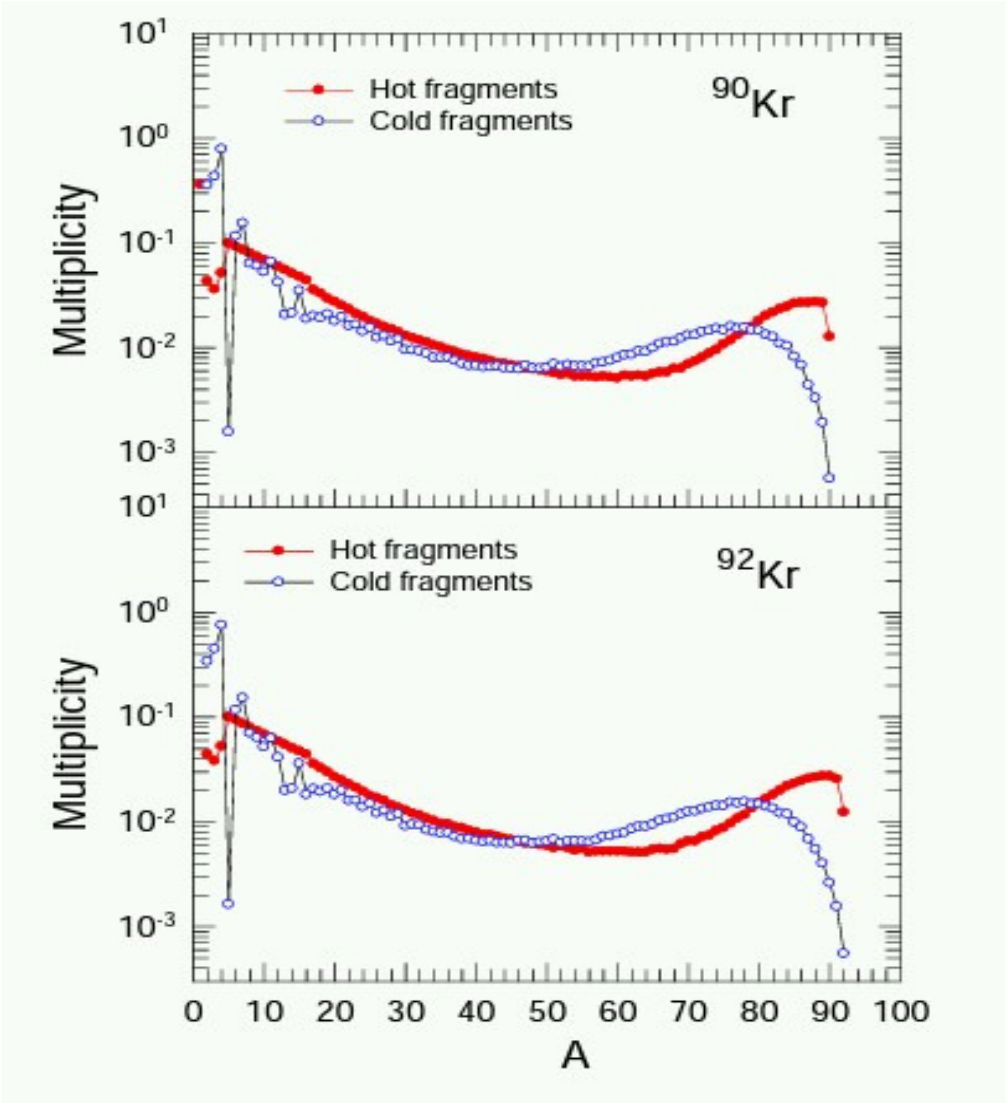

Fig 1 . Hot (red circles) and cold (blue empty circles) fragments for ^{90}Kr and ^{92}Kr

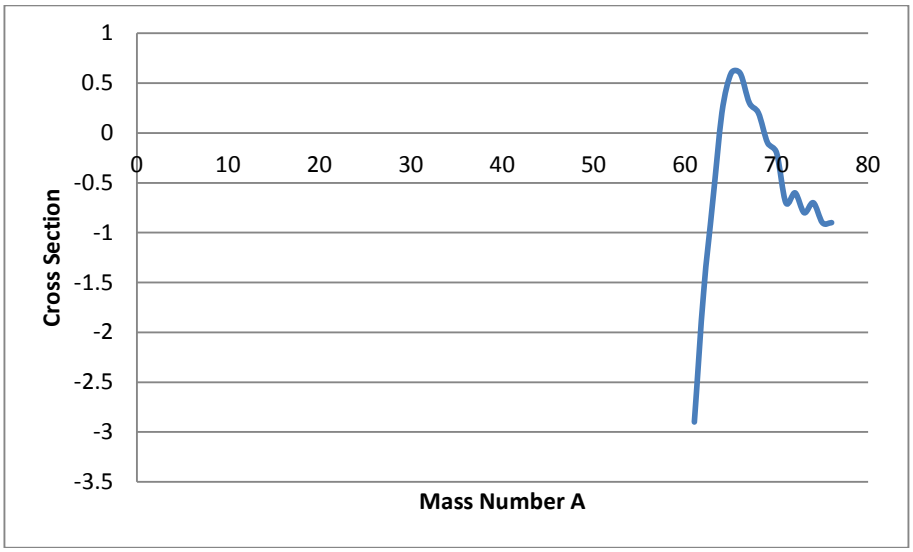

2A: Graph of cross section versus mass number of Theoretical Result for ^{90}Kr

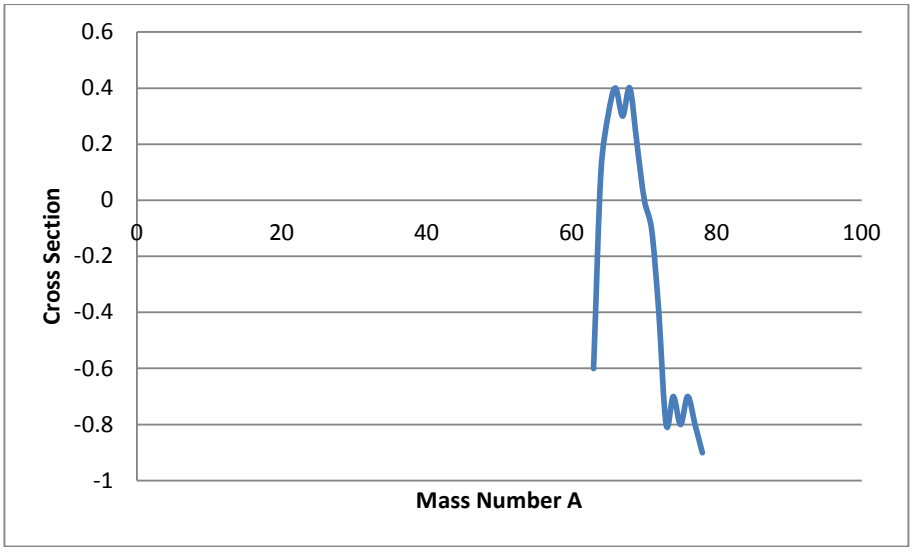

2B: Graph of cross section versus mass number of Theoretical Result for ^{92}Kr

International Journal of Science and Advanced Innovative Research
ISSN: 2536-7315 (Print) 2536-7323 (Online)
Volume 5, Number 1, March, 2020
http://www.casirmediapublishing.com

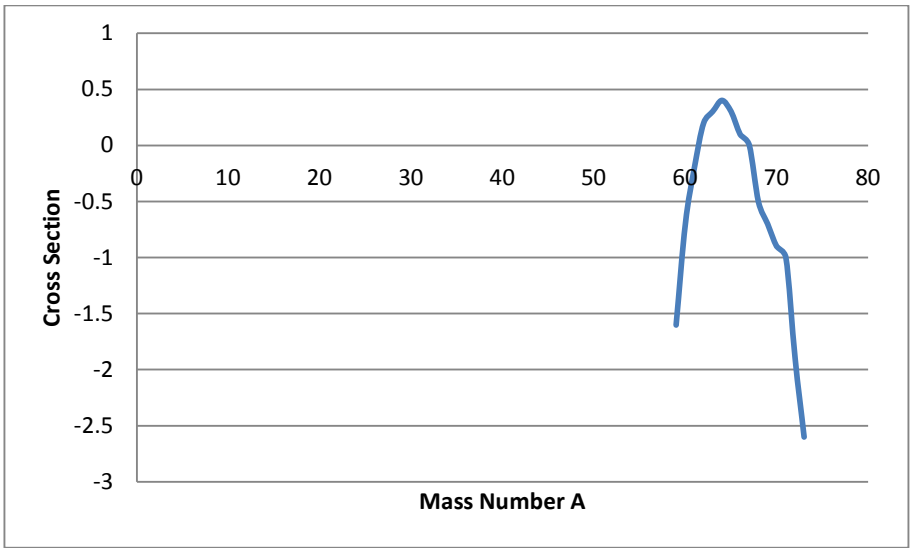

2C: Graph of cross section versus mass number of Experimental Result for ^{90}Kr

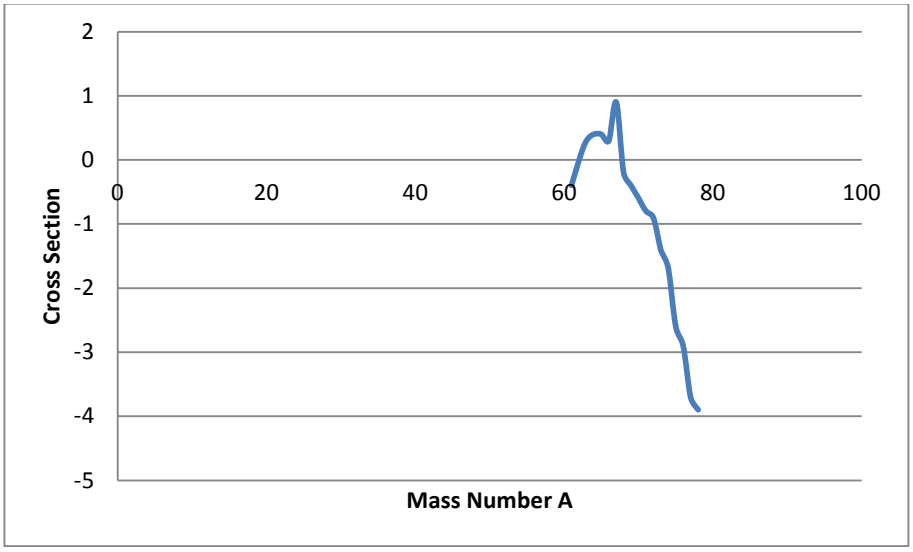

2D: Graph of cross section versus mass number of Experimental Result for ^{92}Kr

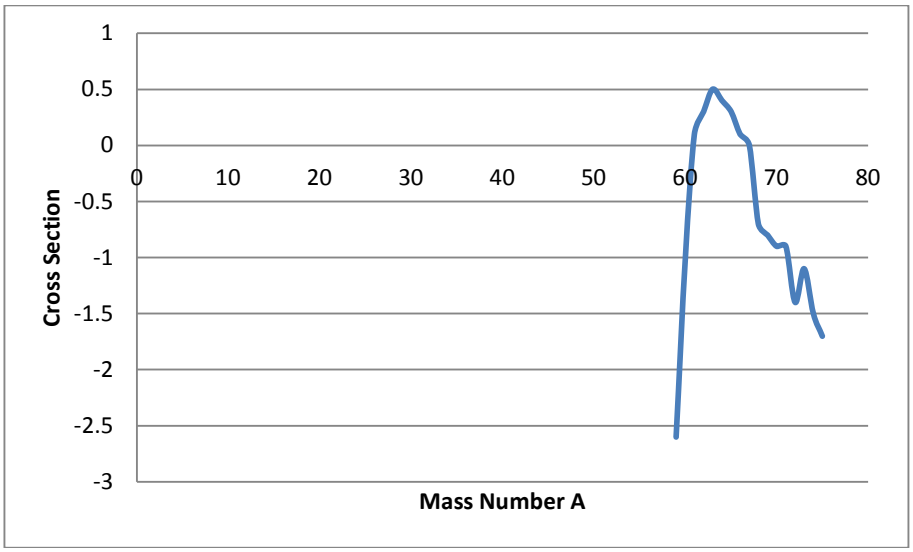

3A: Graph of cross section versus mass number of Theoretical Result for ^{92}Kr if $Z=29$

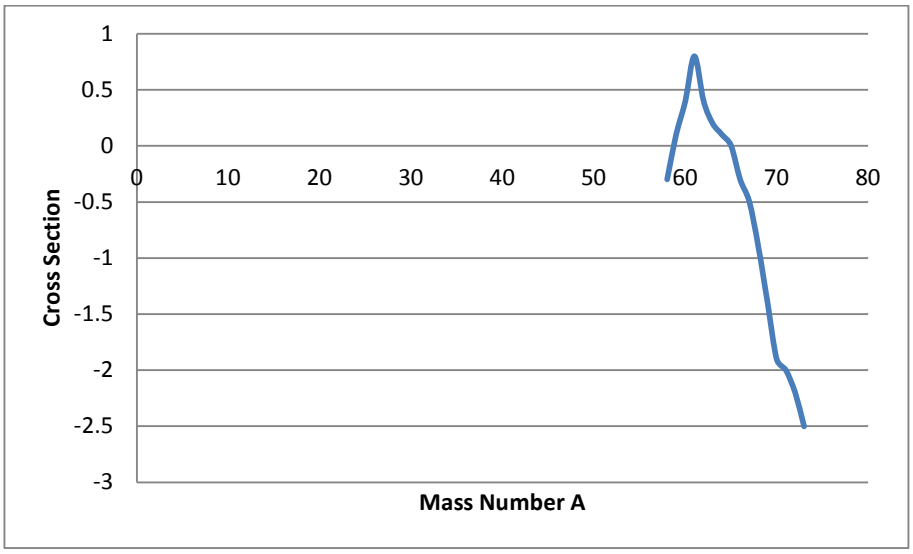

3B: Graph of cross section versus mass number of Experimental Result for ^{92}Kr if $Z=29$

DISCUSSIONS

Fig 1 indicates the results achieved from the current calculation for the hot and cold fragment. The higher panel indicate the average multiplicity of hot and cold fragment from the instrument of sources of ^{90}Kr and lower panel for the more neutron-rich ^{92}Kr. Hot and cold distribution is simply due to the fact that the mass of a hot fragment is reduced after the particle emission. Calculations were performed for iterations and the parameter determined in

for relativistic collisions. The approach can be applied to reproduce the experimental data for the intermediate energy nuclear collisions. In fig 2a, 2b, 2c and 2d, comparing the predicted production cross-section values for the fragments with $Z=30$ with experimental data measured. The normalization results obtained according to the experimental cross-section have been carried out. The results for normalization factors of theoretical event for the fragments of ^{92}Kr with $Z=30$ and similar procedure is applied for the fragment of ^{90}Kr. When one compared the results with experimental data, one may see that the overestimates the fragment yields at the neutron rich side of the isotopic curves. The reason is that experimental isotopic yields were not fully taken into account due to the filters used during the measurement. While on the other hand, it seen that the predicated curves are located under the experimental ones at proton rich side. Fig. 3a and 3b, shows the results for the lighter fragment with $Z=29$ emitted from ^{92}Kr. The calculated and experimental results show satisfactory agreement when compared to fig 2a, 2b, 2c and 2d.

CONCLUSION

It has been observed a satisfactory agreement between the data given in table 1 and 2. It was demonstrated that neutron-rich sources provide more neutron-rich fragment production in the reactions near Coulomb barrier. The kind of reactions, the excitation energy deposited in the sources may drop the particle evaporation threshold.

REFERENCE

[1] Patrignani C. (2016): Review of Particle Physics. Chinese Physics C. 40 (10): 100001. p. 768
[2] Penzes W. B. (2009): Time Line for the Definition of the Meter. National Institute of Standards and Technology, 9th edition, pp 234-243.
[3] Burdun G. D. (1958): On the new determination of the meter" (PDF). Measurement Techniques. 1 (3): 259–264.
[4] Kimothi S. K. (2002): The uncertainty of measurements: physical and chemical metrology: impact and analysis. American Society for Quality. p. 122.
[5] Gibbs P (1997): The speed of light measured. New York Publisher, Vol. 7th, pp 235-238.
[6] Weast R (1984): Modern Physics. Boca Raton, Florida: C&R Company Publishing. pp. E110.
[7] Botvina A. S., Iljinov A. S., Mishustin I. N., Bondorf J. P, Donangelo R. and Sneppen K (1987): Nuclear Physics. 1st edition, pp 475, 663-686.